Supplemental Material

Intrinsic Defect Physics in B-Site Columnar-Ordered Halide Double Perovskites $Cs_2AgPdBr_5$

Wenjun Chu,[a] Xinbo Ma[a] and Zhenyu Li[*,b]

[a]Hefei National Research Center for Physical Sciences at the Microscale, University of Science and Technology of China, Hefei 230026, Anhui, China

[b]Key Laboratory of Precision and Intelligent Chemistry, University of Science and Technology of China, Hefei 230026, Anhui, China

email: zyli@ustc.edu.cn

Table S1. Comparison of the cubic equilibrium lattice parameters (a) and band gaps (E_g) between calculated and experimental results[1] for Cs_2AgPdX_5 (X = Cl, Br) and $Cs_2AgPtCl_5$.

Systems	a(Å)		E g(eV)		
	Cal.	Exp.	Cal. (without SOC)	Cal. (with SOC)	Exp.
$Cs_2AgPdCl_5$	7.49	7.38	1.46	1.47	1.55
$Cs_2AgPdBr_5$	7.87	7.75	1.33	1.34	1.33
$Cs_2AgPtCl_5$	7.52	7.41	1.83	1.63	1.77

Table S2. $\Delta\mu_i$ values for different chemical growth environments as marked in the phase diagram, for $Cs_2AgPdBr_5$.

Chemical environment	$\Delta\mu_{Ag}$ (eV)	$\Delta\mu_{Cs}$ (eV)	$\Delta\mu_{Pd}$ (eV)	$\Delta\mu_{Br}$ (eV)
A	-0.3	-3.13	-0.08	-0.836
B	-0.6	-3.38	-0.60	-0.572
C	-0.9	-3.57	-1.06	-0.344

Table S3. Calculated the carrier effective masses and the effective density of states for Cs_2AgPdX_5 (X = Cl, Br).

	m_e^* (m_0)	m_h^* (m_0)	N_c (cm^{-3})	N_v (cm^{-3})
$Cs_2AgPdCl_5$	0.52	0.98	9.4×10^{18}	2.9×10^{19}
$Cs_2AgPdBr_5$	0.33	0.55	4.9×10^{18}	1.1×10^{19}

Table S4. Pinned fermi level E_F (eV), the hole densities p_0 (cm^{-3}), and electron densities n_0 (cm^{-3}) at the room temperature at three representative chemical potential points A–C in figure 2 for $Cs_2AgPdBr_5$.

chemical potential points	pinned E_F	p_0	n_0
A	0.66	9.4×10^{7}	2.9×10^{7}
B	0.39	3.2×10^{12}	8.6×10^{2}
C	0.08	5.0×10^{17}	5.4×10^{-3}

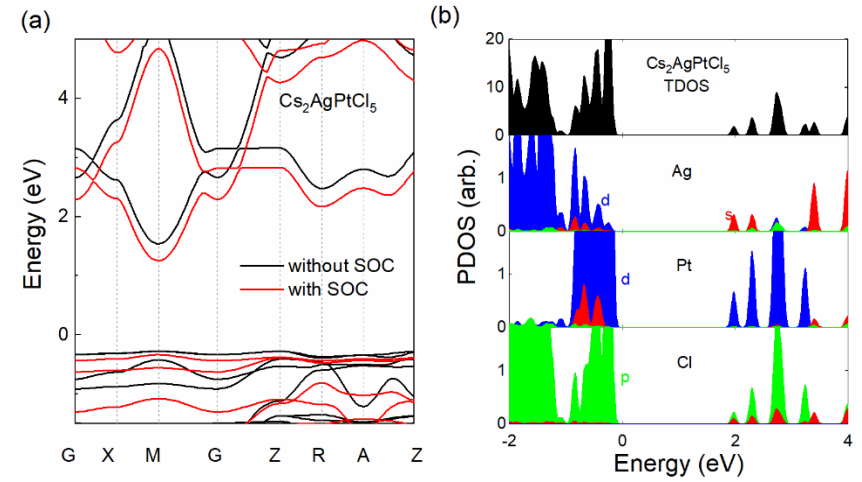

Fig. S1 (a) Band structure and (b) partial density of state of $Cs_2AgPtCl_5$ at the HSE level of theory.

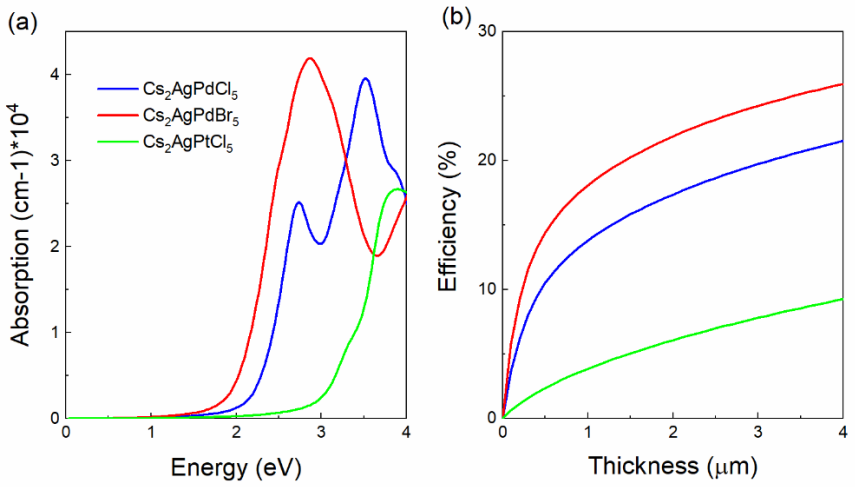

Fig. S2 (a) Optical absorption coefficient vs incident photon energy and (b) limit of efficiency vs film thickness at 298 K for Cs_2AgPdX_5 (X = Cl, Br) and $Cs_2AgPtCl_5$ calculated at the HSE level of theory.

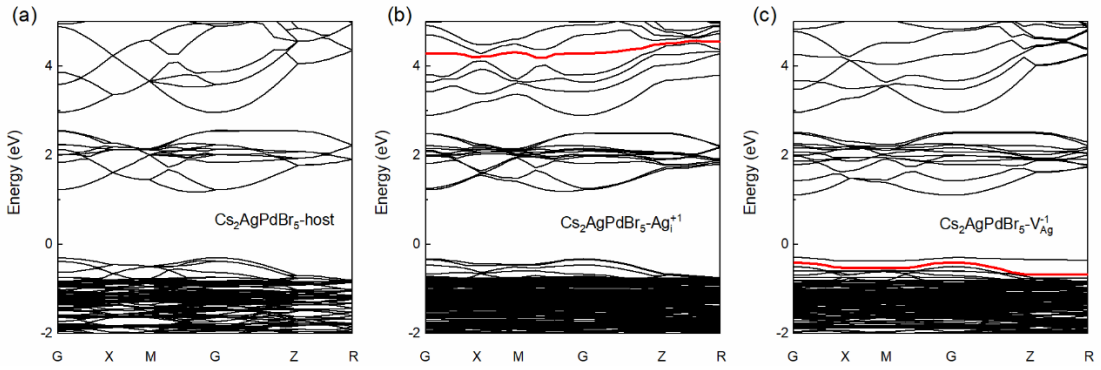

Fig. S3 Band structures of (a) host, (b) $\mathrm{Ag_i^{+1}}$ and (c) $\mathrm{V_{Ag}^{-1}}$ at the HSE level of theory.

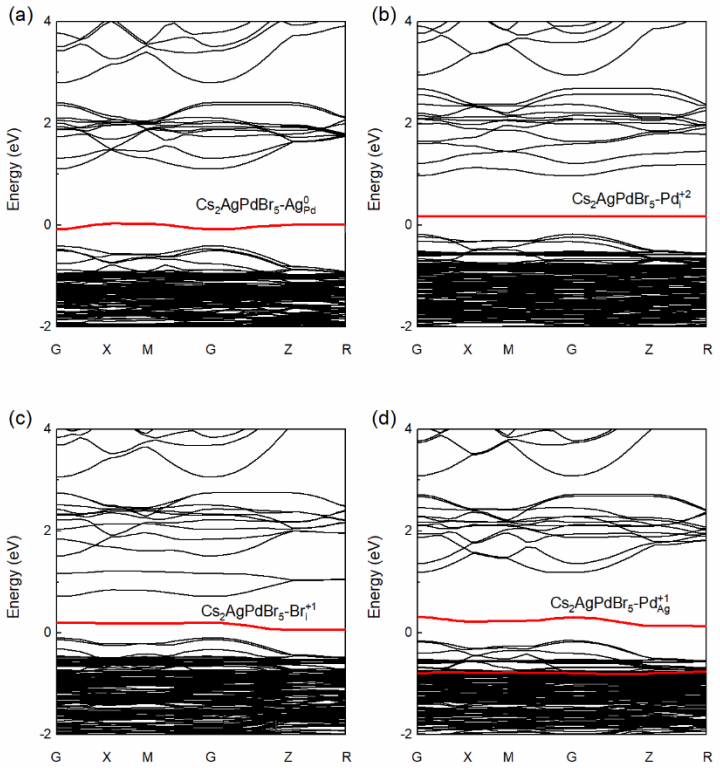

Fig. S4 Band structures of (a) $\mathrm{Ag_{Pd}^{0}}$, (b) $\mathrm{Pd_i^{+2}}$, (c) $\mathrm{Br_i^{+1}}$, and (d) $\mathrm{Pd_{Ag}^{+1}}$ at the HSE level of theory, respectively.

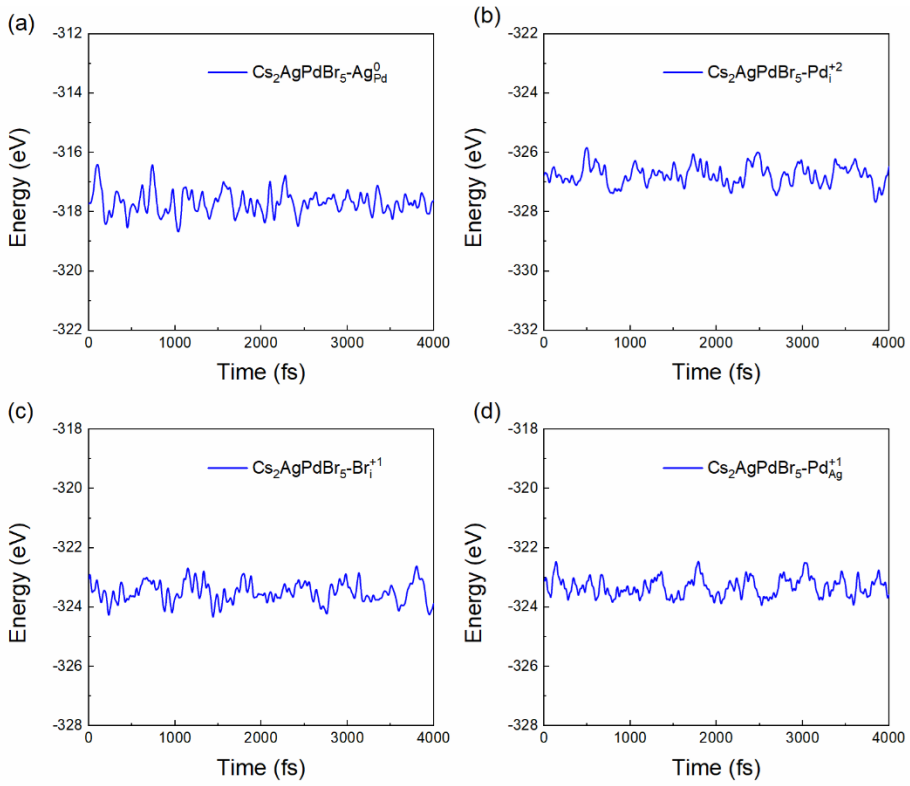

Fig. S5 The Fluctuation of total potential energy at Gamma point for $Cs_2AgPdBr_5$ during the AIMD simulation at 300 K.

References

1 G. Ji, C. Han, S. Hu, P. Fu, X. Chen, J. Guo, J. Tang and Z. Xiao, *J. Am. Chem. Soc.*, 2021, **143**, 10275-10281.